

Adaptive Control of a Robot Carrying a Time-Varying Payload

Prabhakar R. Pagilla¹

Biao Yu

School of Mechanical and Aerospace Engineering
Oklahoma State University
Stillwater, OK 74075

Abstract. In this paper, we consider adaptive control of a robot carrying a time-varying payload. The robot dynamic model and its properties are given for time-varying payloads. This dynamic model and its properties are different when compared with a robot dynamic model with constant payload. A compact parameterization of the dynamics is obtained based on the payload being parameterized by a group of known bounded functions and unknown constant parameters. Based on this parameterization, a passivity-type adaptive control law is proposed for the robot with time-varying payload. Stability of the closed-loop system with the proposed adaptive controller is shown. An experimental platform consisting of a two-link robot with a time-varying payload has been developed. The experimental platform mimics pouring/filling operations using a robot. Typical experimental results are shown and discussed.

1 Introduction

Research in the area of trajectory tracking control of mechanical systems has been widespread. The trajectory tracking control problem of the robot manipulators is an important research topic since many of the tasks such as material handling, transportation, part assembly, etc. performed by robot manipulators involve such a problem. Many control designs exist in literature that work well with both known and unknown constant parameters. However, in many situations, some of the unknown parameters, especially the mass of the payload or the mass of the links, may be time-varying. Examples of such operations include pouring and filling operations. Control algorithms exist based on the assumption that the parameters are constant or slowly time-varying. However, if the change is significant then the robot dynamic model for constant parameters cannot be used to describe the dynamic behavior. Limited work in the area of time-varying mechanical systems exists in the literature. Constrained Lagrangian dynamics of discrete systems

can be found in [1, 2]. In [3], a robust switching controller is designed for the time-varying parameter model of the robot manipulators performing path tracking tasks. Properties of the element product of matrices is used to isolate the time-varying parameters from the inertia matrix. A robust adaptive control for robot manipulators consisting of slowly time-varying parameters is presented in [4]. For the constant parameter case, we refer to [7] for several adaptive motion control designs that appeared in the literature.

Dynamic model for time-varying mechanical systems and preliminary experimental results for robot carrying a time-varying payload were given in [8]. In this paper, we introduce the concept of time-scaling to eliminate the boundedness problem of time-varying parameters in [8]. The time-varying payload in the experiments consists of a vessel on the robot end-effector into which water is poured in/out during motion to create the time-varying nature. Due to the time-varying payload, the regressor matrix in the adaptation law depends on time explicitly, we introduce a notion of time-scaling by mapping a cycle period of the desired trajectory to the unit interval, $[0,1]$. The proposed design can be applied to filling/pouring operations in industry. To test the adaptive controller we design an experimental platform to mimic filling/pouring operations. This platform consists of a two-link robot with a time-varying payload. The time-varying nature of the payload is obtained by pumping fluid in/out of a cylindrical vessel carried by the robot manipulator. Successful experimental results validate the proposed adaptive designs.

The rest of the paper is organized as follows. In Section 2, the dynamic model for time-varying mechanical system and its properties are given. The proposed adaptive controller is given in Section 3, and stability of the closed-loop system is shown. In Section 4, experimental platform is described. Dynamic equations and adaptive controller for the two-link robot example are given in Section 4.1 and

¹pagilla@ceat.okstate.edu

Section 4.2. In Section 4.3, we propose the idea of time-scaling. Comparative experimental results are given in Section 4.4. Section 5 gives conclusions of this work.

2 Dynamics

The dynamic equations of a robot with time-varying payload [8] are given by

$$M(q, m_p)\ddot{q} + C(q, \dot{q}, m_p)\dot{q} + F(q, \dot{m}_p)\dot{q} + g(q, m_p) = \tau \quad (1)$$

where $m_p(t)$ is the time-varying payload, $M(q, m_p)$ is the inertia matrix, $C(q, \dot{q}, m_p)$ is the Coriolis matrix, τ is a vector of external control inputs, $g(q, m_p)$ is the gravity vector, and $F(q, \dot{m}_p)$ is an additional term that appears in the dynamics because of the time-varying payload. A complete derivation of the dynamics given by equation (1) can be found in [8]. In this section, we briefly state the well known properties of the dynamic model and emphasize the variations that are obtained due to the additional term in the time-varying model.

Property 1: The inertia matrix, $M(q, m_p)$, is a symmetric positive definite matrix. This matrix for all system configurations is bounded from above and below assuming that m_p is bounded.

Property 2: The matrix $F(q, \dot{m}_p)$ is a symmetric matrix, which is a consequence of the symmetry of the inertia matrix.

Property 3: The matrix $\dot{M}(q, m_p) - 2C(q, \dot{q}, m_p) - F(q, \dot{m}_p)$ is skew-symmetric. Notice that the skew-symmetry property for the time-varying case is different from that of the time-invariant case.

Property 4: The dynamic equation (1) is linear in the unknown parameters. This property may be expressed as

$$M(q, m_p)\ddot{q} + C(q, \dot{q}, m_p)\dot{q} + F(q, \dot{m}_p)\dot{q} + g(q, m_p) = Y(q, \dot{q}, \ddot{q})\theta(t) \quad (2)$$

where $\theta^T(t) := [\theta_0^T, m_p(t), \dot{m}_p(t)]$ is the parameter vector, consisting of constant inertial parameters of the robot (θ_0) and the time-varying payload (m_p) and its derivative (\dot{m}_p). $Y(q, \dot{q}, \ddot{q})$ is the regressor matrix, which depends on the joint variables, joint velocities and joint acceleration.

3 Adaptive Control

Let $q_d(t)$ be the desired trajectory. We assume that $q_d(t)$ is twice continuously differentiable. Let $e = q(t) - q_d(t)$ be the joint tracking error, and $e_{vp} = \dot{e} + \Lambda e$ be the reference velocity error. Consider the control law, τ , given by

$$\tau = Y(q, \dot{q}, \ddot{q}_r)\hat{\theta} - K_{vp}e_{vp} \quad (3)$$

where $\dot{q}_r = \dot{q}_d - \Lambda e$, K_{vp} and Λ are positive definite gain matrices, $\hat{\theta}$ is the estimate of θ , and $Y(q, \dot{q}, \ddot{q}_r)$ is given by

$$Y(q, \dot{q}, \ddot{q}_r)\hat{\theta} = \widehat{M}(q, \hat{m}_p)\ddot{q}_r + \widehat{C}(q, \dot{q}, \hat{m}_p)\dot{q}_r + \frac{1}{2}\widehat{F}(q, \hat{m}_p)\dot{q}_r + \frac{1}{2}\widehat{F}(q, \hat{m}_p)\dot{q} + \hat{g}(q, \hat{m}_p)$$

where \widehat{A} represents the estimate of A . Consider the following modification using the linear parameterization property,

$$Y(q, \dot{q}, \ddot{q})\theta = Y_0(q, \dot{q}, \ddot{q})\theta_0 + Y_1(q, \dot{q}, \ddot{q})m_p(t) + Y_2(q, \dot{q}, \ddot{q})\dot{m}_p(t) \quad (4)$$

where θ_0 is a vector of constant inertial parameters of the robot.

$$Y(q, \dot{q}, \ddot{q}_r)\hat{\theta} = Y_0(q, \dot{q}, \ddot{q}_r)\hat{\theta}_0 + Y_1(q, \dot{q}, \ddot{q}_r)\hat{m}_p(t) + Y_2(q, \dot{q}, \ddot{q}_r)\hat{\dot{m}}_p(t) \quad (5)$$

Now, we assume that the time-varying parameter vector $m_p(t)$ is parameterized as follows:

$$m_p(t) = k_1 f_1(t) + k_2 f_2(t) + \dots + k_n f_n(t) \quad (6)$$

where k_1, k_2, \dots, k_n are unknown constants, and $f_1(t), f_2(t), \dots, f_n(t)$ are known bounded functions.

3.1 Closed-loop Dynamics

Substituting the control law (3) into the dynamic equations (1), and after simplifying we obtain

$$M(q, m_p)\dot{e}_{vp} + C(q, \dot{q}, m_p)e_{vp} + \frac{1}{2}F(q, \dot{m}_p)e_{vp} = Y_0(q, \dot{q}, \ddot{q}_r)\tilde{\theta}_0 + \sum_{i=1}^n W_i(q, \dot{q}, \ddot{q}_r, t)\tilde{k}_i \quad (7)$$

where $\tilde{k}_i(t) := \hat{k}_i(t) - k_i$ and

$$W_i(q, \dot{q}, \ddot{q}_r, t) := \{f_i(t)Y_1(q, \dot{q}, \ddot{q}_r) + Y_2(q, \dot{q}, \ddot{q}_r)\frac{df_i(t)}{dt}\} \quad (8)$$

Stability of the closed-loop system can be found in [5].

4 Experiments

The experimental setup consists of a two-degree-of-freedom direct drive manipulator with a cylindrical vessel on the end of the second link. A pipe is connected from the top of vessel to a pump either to pump fluid in or out of the vessel. Pumping of fluid in or out of the vessel during the motion of robot gives the time varying nature for the payload. A sketch of the experimental platform is shown in Figure 1. Details of the experimental platform can be found in [5].

4.1 Dynamic Equations of the Two-Link Robot with Time-Varying Payload

The dynamic equations of the manipulator are given by

$$M(q, m_p)\ddot{q} + C(q, \dot{q}, m_p)\dot{q} + F(q, \dot{m}_p)\dot{q} = \tau, \quad (9)$$

where $q \in \mathbf{R}^2$ is the joint position vector, and $\tau \in \mathbf{R}^2$ are the motor torques. The elements of matrices $M(q, m_p)$, $C(q, \dot{q}, m_p)$, and $F(q, \dot{m}_p)$ are given as follows:

$$\begin{aligned} M_{11} &= p_1 + 2p_2 \cos(q_2) + v_1(q_2)m_p(t) + I_p(t) \\ M_{12} &= p_3 + p_2 \cos(q_2) + v_2(q_2)m_p(t) + I_p(t) \\ M_{21} &= M_{12} \\ M_{22} &= p_3 + v_3m_p(t) + I_p(t) \\ C(\cdot) &= - \begin{bmatrix} \dot{q}_2 p_7 & (\dot{q}_1 + \dot{q}_2) p_7 \\ -\dot{q}_1 p_7 & 0 \end{bmatrix} \\ F(\cdot) &= \begin{bmatrix} v_1(q_2) & v_2(q_2) \\ v_2(q_2) & v_3 \end{bmatrix} \dot{m}_p + \begin{bmatrix} 1 & 1 \\ 1 & 1 \end{bmatrix} \dot{I}_p \end{aligned}$$

where p_1, p_2, p_3 are the constant coupled parameters of the robot that contain masses and inertias of the links and the motors, $m_p(t)$ and $I_p(t)$ are the payload mass and inertia, respectively, $p_7(m_p, q) = (p_2 + l_1 l_2 m_p(t)) \sin(q_2)$, $v_1(q) = l_1^2 + l_2^2 + 2l_1 l_2 \cos(q_2)$, $v_2(q) = l_2^2 + l_1 l_2 \cos(q_2)$, and $v_3 = l_2^2$. The link lengths are represented by l_1 and l_2 . Since the payload is a cylindrical vessel of a fixed diameter, the inertia of the payload $I_p(t) = m_p(t)(R^2/2)$, where R is the radius of the cylindrical vessel. According to the water pump specifications the rated flow rate of the pump is linear within the operating conditions of the pump. This means that the mass of the payload varies according to $m_p(t) = k_1 t$, where k_1 represents the constant water flow rate in or out of the vessel. The dynamics is linear in the unknown parameters,

$$M(q, m_p)\ddot{q} + C(q, \dot{q}, m_p)\dot{q} + F(q, \dot{m}_p)\dot{q} = Y(q, \dot{q}, \ddot{q})\theta \quad (10)$$

Also, $Y(q, \dot{q}, \ddot{q})$ can be decomposed to associate with constant parameters and time-varying payload as

$$Y(q, \dot{q}, \ddot{q})\theta = Y_0(q, \dot{q}, \ddot{q})\theta_0 + Y_1(q, \dot{q}, \ddot{q})m_p(t) + Y_2(q, \dot{q}, \ddot{q})\dot{m}_p(t), \quad (11)$$

where $\theta_0^T = [p_1, p_2, p_3]$. Define $\alpha = R^2/2$, and

$$\begin{aligned} y_{11} &:= v_1(q)\ddot{q}_1 + v_2(q)\ddot{q}_2 - l_1 l_2 \sin(q_2)(\dot{q}_2^2 + 2\dot{q}_1 \dot{q}_2) \\ y_{12} &:= \ddot{q}_1 + \ddot{q}_2; \quad y_{13} := v_2(q)\dot{q}_1 + v_3\dot{q}_2 \\ y_{14} &:= \dot{q}_1 + \dot{q}_2 \\ y_{21} &:= v_2(q)\ddot{q}_1 + v_3\ddot{q}_2 + l_1 l_2 \sin(q_2)\dot{q}_1^2 \\ y_{22} &:= y_{12}; \quad y_{23} := v_2(q)\dot{q}_1 + v_3\dot{q}_2; \quad y_{24} := y_{14} \end{aligned}$$

Then,

$$\begin{aligned} W_1(q, \dot{q}, \ddot{q}, t)k_1 &:= Y_1(q, \dot{q}, \ddot{q})m_p(t) + Y_2(q, \dot{q}, \ddot{q})\dot{m}_p(t) \\ &= \begin{bmatrix} t(y_{11} + \alpha y_{12}) + y_{13} + \alpha y_{14} \\ t(y_{21} + \alpha y_{22}) + y_{23} + \alpha y_{24} \end{bmatrix} k_1 \end{aligned}$$

4.2 Adaptive Controller

The following are the control law and adaptation laws for the two-link robot with a time-varying payload

$$\begin{aligned} \tau &= Y_0(q, \dot{q}, \ddot{q}, \ddot{q}_r)\hat{\theta}_0(t) + W_1(q, \dot{q}, \ddot{q}, \ddot{q}_r, t)\hat{k}_1(t) \\ &\quad - K_{vp}e_{vp} \end{aligned} \quad (12)$$

$$\dot{\hat{\theta}}_0(t) = -\Gamma_0 Y_0^T(q, \dot{q}, \ddot{q}, \ddot{q}_r)e_{vp} \quad (13)$$

$$\dot{\hat{k}}_1(t) = -\Gamma_1 W_1^T(q, \dot{q}, \ddot{q}, \ddot{q}_r)e_{vp} \quad (14)$$

where K_{vp} is the positive definite feedback gain matrix, Γ_i is the adaptation gain matrix and

$$Y_0(q, \dot{q}, \ddot{q}, \ddot{q}_r) = \begin{bmatrix} \ddot{q}_{r1} & \ddot{q}_{r2} & Y_{013} \\ 0 & \ddot{q}_{r1} + \ddot{q}_{r2} & Y_{023} \end{bmatrix} \quad (15)$$

$$W_1(q, \dot{q}, \ddot{q}, \ddot{q}_r, t) = \begin{bmatrix} t(z_{11} + \alpha z_{12}) + z_{13} + \alpha z_{14} \\ t(z_{21} + \alpha z_{22}) + z_{23} + \alpha z_{24} \end{bmatrix} \quad (16)$$

where $Y_{013} := 2c_2(\ddot{q}_{r1} + \ddot{q}_{r2}) - (\dot{q}_1 \dot{q}_{r2} + \dot{q}_{r1} \dot{q}_2 + \dot{q}_2 \dot{q}_{r2})s_2$, $Y_{023} := c_2 \ddot{q}_{r1} + s_2 \dot{q}_1 \dot{q}_{r1}$, and

$$\begin{aligned} z_{11} &:= v_1(q)\ddot{q}_{r1} + v_2(q)\ddot{q}_{r2} \\ &\quad - l_1 l_2 \sin(q_2)(\dot{q}_2 \dot{q}_{r2} + \dot{q}_1 \dot{q}_{r2} + \dot{q}_{r1} \dot{q}_2) \\ z_{13} &:= \frac{1}{2}(v_2(q)\dot{q}_1 + v_3\dot{q}_2) + \frac{1}{2}(v_2(q)\dot{q}_{r1} + v_3\dot{q}_{r2}) \\ z_{14} &:= \frac{1}{2}(\dot{q}_1 + \dot{q}_2) + \frac{1}{2}(\dot{q}_{r1} + \dot{q}_{r2}) \\ z_{21} &:= v_2(q)\ddot{q}_{r1} + v_3\ddot{q}_{r2} + l_1 l_2 \sin(q_2)\dot{q}_1 \dot{q}_{r1} \\ z_{23} &:= \frac{1}{2}(v_2(q)\dot{q}_1 + v_3\dot{q}_2) + \frac{1}{2}(v_2(q)\dot{q}_{r1} + v_3\dot{q}_{r2}) \\ z_{12} &:= \ddot{q}_{r1} + \ddot{q}_{r2}; \quad z_{22} := z_{12}; \quad z_{24} := z_{14} \end{aligned}$$

Notice that the regressor matrix $W_1(q, \dot{q}, \ddot{q}, \ddot{q}_r, t)$ contains time explicitly. Recall that $m_p(t) = k_1 t$, this means that according to the parameterization (6) $f_1(t) = t$. The function $f_1(t)$ in this case is unbounded. To avoid this problem, we use the notion of time-scaling, which is described in detail in the section below.

4.3 Time-Scaling

We first consider the general case where the functions are given by, $f_i(t) = t^i$, i.e., the time-varying payload is $m_p(t) = k_1 t + k_2 t^2 + \dots + k_n t^n$. Then the adaptation laws for k_i are given by

$$\dot{\hat{k}}_i(t) = -\Gamma_i W_i^T(q, \dot{q}, \ddot{q}, \ddot{q}_r, t)e_{vp} \quad (17)$$

where

$$W_i(\cdot) = \{t^i Y_1(q, \dot{q}, \ddot{q}_r, \ddot{q}_r) + Y_2(q, \dot{q}, \ddot{q}_r, \ddot{q}_r) i t^{i-1}\}$$

Notice that when the adaptation is run for a long time (i.e. t large), then any small error e_{vp} significantly magnifies the adaptation law (17). This is basically due to the fact that the functions f_i are not bounded. During experiments, we have noticed severe oscillation of \hat{k}_i when t becomes large. To remedy this situation we map our entire time interval into a unit interval $[0, 1]$. We do this as follows. Suppose the robot is performing a periodic desired trajectory with a period T . Then the time-varying payload can be written as

$$m_p(t) = \sum_{i=1}^n (k_i T) + (k_i T^i) \left(\frac{t}{T}\right)^i \quad (18)$$

Notice that $t/T \in [0, 1]$. Define $k'_i = k_i T^i$. Then the adaptation laws for k'_i are given by

$$\dot{\hat{k}}'_i(t) = -\Gamma_i W_i'^T(q, \dot{q}, \ddot{q}_r, \ddot{q}_r, t/T) e_{vp} \quad (19)$$

where

$$W_i'(\cdot) = \left(\frac{t}{T}\right)^i Y_1(q, \dot{q}, \ddot{q}_r, \ddot{q}_r) + Y_2(q, \dot{q}, \ddot{q}_r, \ddot{q}_r) i \left(\frac{t}{T}\right)^{i-1}$$

It should be observed that the modification of the adaptation law does not affect the stability analysis conducted in Section 3. It just merely maps the cycle period to the unit interval, $[0, 1]$. Also, $\hat{k}_i(t)$ and $\hat{k}'_i(t)$ are related by a constant T^i , that is $\hat{k}_i(t) = (1/T^i) \hat{k}'_i(t)$. Similarly, if the time-varying payload $m_p(t)$ is given by (6), then we can normalize it in some sense, for example

$$m_p(t) = k'_1 g_1(t) + k'_2 g_2(t) + \dots + k'_n g_n(t)$$

where $k'_i \|f_i(t)\|$, and $g_i(t) = f_i(t) / \|f_i(t)\|$.

For the example considered, where the payload mass is linearly time-varying, that is $m_p(t) = k_1 t$, define $k'_1 = k_1 T$. Then, the adaptation law for k'_1 is given by

$$\dot{\hat{k}}'_1(t) = -\Gamma_1 W_1'^T(q, \dot{q}, \ddot{q}_r, \ddot{q}_r, t/T) e_{vp} \quad (20)$$

where

$$W_1'(\cdot) = \begin{bmatrix} \frac{t}{T}(z_{11} + \alpha z_{12}) + z_{13} + \alpha z_{14} \\ \frac{t}{T}(z_{21} + \alpha z_{22}) + z_{23} + \alpha z_{24} \end{bmatrix}$$

Notice that the adaptive control law (12) is convenient if several cycles of a periodic trajectory are implemented. Since accumulation of the payload

mass should be taken into account after every cycle, the control law can be simply changed to

$$\begin{aligned} \tau(j) &= Y_0(q, \dot{q}, \ddot{q}_r, \ddot{q}_r) \hat{\theta}_0(t) + W_0(q, \dot{q}, \ddot{q}_r, \ddot{q}_r) \beta(j-1) \\ &\quad + W_1(q, \dot{q}, \ddot{q}_r, \ddot{q}_r, t) \hat{k}'_1(t) - K_{vp} e_{vp} \\ \beta_j &= \beta_{j-1} + \int_0^1 \hat{k}'_{1,j-1}(\omega) d\omega \end{aligned} \quad (21)$$

where $\beta(0) = 0$, $\hat{k}'_{1,0} = 0$, and

$$W_0(q, \dot{q}, \ddot{q}_r, \ddot{q}_r) = \begin{bmatrix} z_{11} + \alpha z_{12} \\ z_{21} + \alpha z_{22} \end{bmatrix},$$

and j denotes the cycle index, that is $j = 1$ represents the first cycle, and so on. Notice that $\beta(j)$ is updated only once at the beginning of the cycle. It is basically the amount of payload added/removed in cycle j to the container, which represents a constant payload for the $(j+1)$ -th cycle. The control law (21) decouples the constant parameters from the time-varying payload, i.e. the adaptation laws for the constant parameters of the robot are not affected by the adaptation laws of the time-varying payload, and vice-versa. The experimental results clearly validate this aspect.

4.4 Experimental Results

Extensive experiments were conducted using the proposed adaptive controller. Results from typical experiments are presented here. Three groups of experiments are presented:

- **Group I:** passivity-based controller without adaptation,
- **Group II:** proposed adaptive controller without time scaling, and
- **Group III:** proposed adaptive controller with time scaling.

Experiments of pumping water into and out of the cylindrical vessel were conducted for three cases. Similar results were obtained for both pumping water into the vessel and out of the vessel. We show results for pump-in case only due to lack of space. Fig. 3 through 4 show the L_2 norm of the joint position errors for the pump-in case. The desired trajectory for the robot end-effector is a circle with a period of four seconds. Servo sampling rate of four milli-seconds is used in the experiments. It takes about ten cycles to fill the vessel with water. For safety of not spilling the water during the motion of the robot we use 6-8 cycles.

For **Group I** experiments, Fig. 2 indicates that the tracking errors increase with the time-varying payload.

For **Group II** experiments, Fig. 3 indicates that the tracking errors decrease for first several cycles and then increase as t increases. Since time t explicitly appears in the regressor matrix in the adaptation law, small error in e_{vp} is magnified when t is larger.

For **Group III** experiments, the L_2 norm of the tracking errors for each cycle, the payload estimate and the robot constant inertial parameters estimates are given in Figures 4, 5, and 6, respectively. For this group the tracking errors decrease after each cycle. The tracking errors are bounded by about one-fourth of a degree for joint 1 and one-half of a degree for joint 2. The true values of the constant robot inertial parameters without any payload are $p_1 = 3.4$, $p_2 = 0.4$, and $p_3 = 0.3$. We assume no initial knowledge of $m_p(t)$, and 50% uncertainty in the constant robot inertial parameters. From Figure (5) it can be observed that time-varying payload estimate converges to the true value. The top plot in Figure (5) shows the flow rate k_1 and the bottom plot shows the payload mass $m_p(t)$.

Remarks:

- Parameter estimates are influenced by low velocity friction at the beginning and the end of each cycle. The peaks in robot inertial parameter estimates, Figure 6, correspond to peaks in desired acceleration, this is due to the fact that the regressor contains the desired acceleration. Also, notice that k_1 estimates are affected at the beginning and end of the cycle. This may be primarily due to the presence of low-velocity friction, since in the middle of the cycle the estimate of k_1 is flat when the velocity is higher.
- The estimation of time-varying payload is independent of the estimation of the constant robot parameters. We conducted experiments with no payload (container empty) and with full payload (container filled with water), and observed the estimation of parameters to be of similar pattern as shown in Figures (5) and (6).
- Robot parameter estimates are influenced by the desired acceleration whereas the k_1 estimate is influenced by the desired velocity. This can be deduced from the corresponding regressors, i.e. $Y_0(q, \dot{q}, \ddot{q}_r)$ given by (15), and $W_1(q, \dot{q}, \ddot{q}_r, t)$ given by (16). Notice that $Y_0(q, \dot{q}, \ddot{q}_r)$ has elements involving desired acceleration. The elements in $W_1(q, \dot{q}, \ddot{q}_r, t)$ which have the desired acceleration term are multiplied by t .
- Experiment results with typical robot adaptive control algorithms designed for the con-

stant parameter show that the estimates for constant parameters cannot pick up the time-varying payload. The tracking errors increase due to the time-varying payload.

5 Conclusions

Adaptive control of a robot carrying a time-varying payload is considered in this paper. Dynamic model of a robot with time-varying payload is given. Based on this dynamic model we developed an adaptive controller assuming that the time-varying parameters are linearly parameterized by a group of bounded time functions and constant parameters. An experimental platform that mimics filling/pouring operations using robot manipulators has been designed to test the proposed adaptive controller. Due to the time-varying nature of the payload the regressor matrix in the adaptation laws may contain time explicitly. This causes parameter convergence problems for large time, even when small oscillatory errors appear. If the time-varying payload is not bounded, we proposed a technique of time-scaling that maps each cycle of the trajectory to a unit interval. Comparative experimental results validate the effectiveness of the proposed adaptive control design. The experiments conducted in this paper use a linear rate of change of payload mass. Our future research in this area will focus on different rates of change of payload mass.

References

- [1] R.M. Rosenberg, Analytical dynamics of discrete systems. *Plenum Press*, NY, 1977.
- [2] D.T. Greenwood, Classical Dynamics *Prentice-Hall, Inc*, Englewood Cliffs, NJ, 1977.
- [3] Y.D. Song and R.H. Middleton, Dealing with the time-varying parameter problem of robot manipulators performing path tracking tasks. *IEEE Trans. Auto. Contr.*, 37(10):1597–1601, 1992.
- [4] J.S. Reed and P.A. Ioannou, Instability analysis and robust adaptive control of robotic manipulators. *IEEE Trans. Rob. and Auto.*, 5(3):381–386, 1989.
- [5] P.R. Pagilla, B. Yu, and K.L. Pau, Adaptive control of time-varying mechanical systems: Modeling, controller design and experiments, to appear in the *IEEE/ASME Transactions on Mechatronics*, 2000.
- [6] N. Sadegh and R. Horowitz, Stability and Robustness Analysis of a Class of Adaptive Controllers for Robot Manipulators, *IEEE Trans. Rob. and Auto.*, 5(3):381–386, 1989.
- [7] J.J. Slotine and W. Li. *Applied Nonlinear Control*. Prentice Hall, 1991.
- [8] P.R. Pagilla, K.L. Pau, and B. Yu, Adaptive control of time-varying mechanical systems: Modeling, controller design and experiments, in the *1999 IEEE International Conference on Robotics and Automation*, 1999.

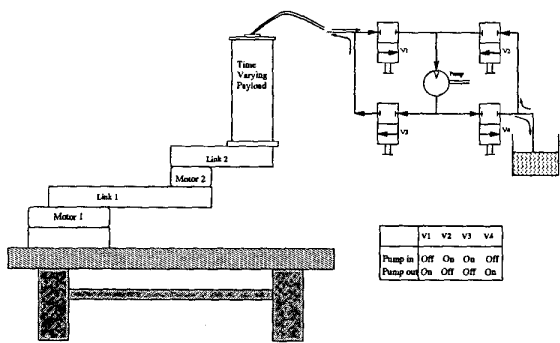


Figure 1: Experimental Setup

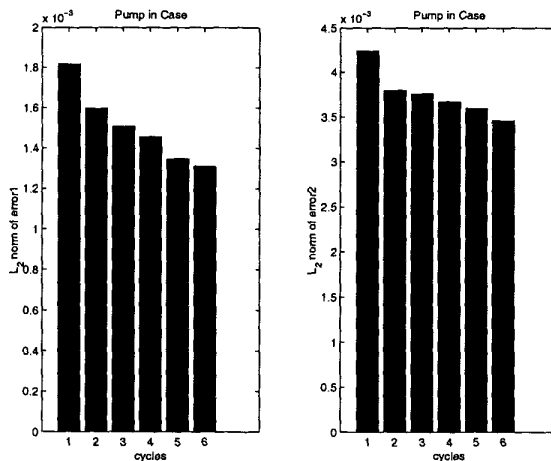


Figure 4: L_2 norm of joint position errors (Group III)

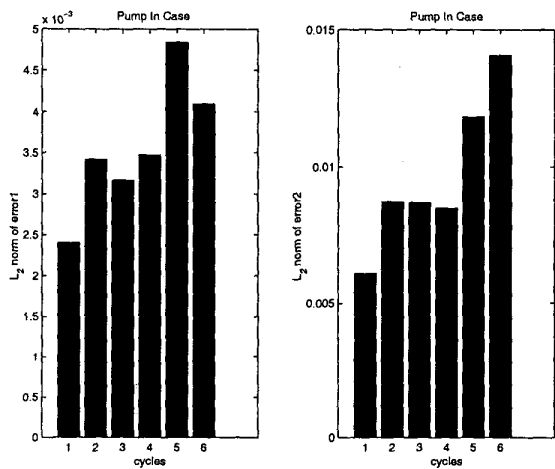


Figure 2: L_2 norm of joint position errors (Group I)

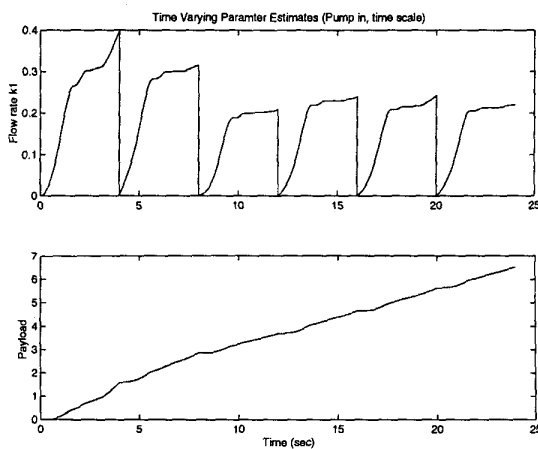


Figure 5: Payload estimation (Group III)

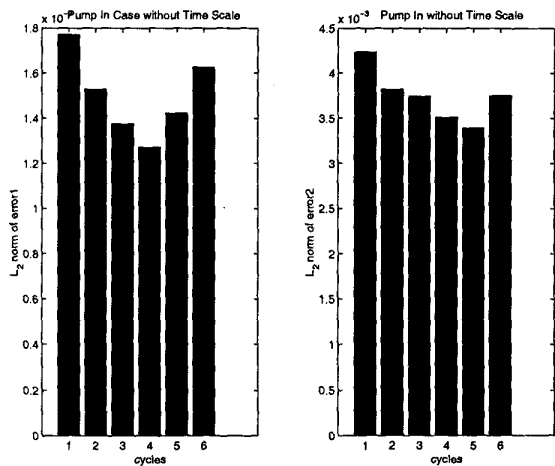


Figure 3: L_2 norm of joint position errors (Group 2)

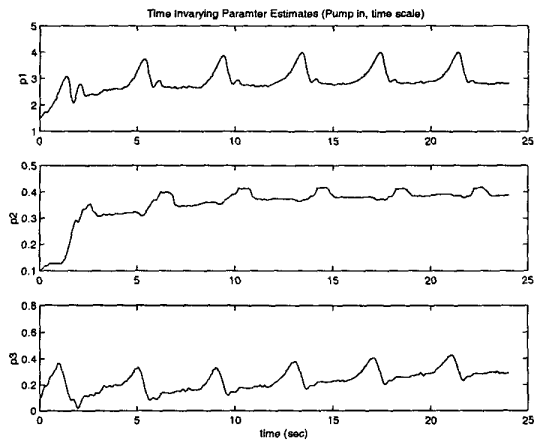


Figure 6: Robot parameters estimation (Group III)